HIROSHIMA MATH. J.
23 (1993), 417–448

Numerical treatment on the behavior of interfaces in oil-reservoir problems

Tatsuyuki NAKAKI

(Received January 18, 1992)

1. Introduction

Nonlinear problems arising in industrial mathematics have been extensively investigated for a long time. In the field of the reservoir engineering, there appear interesting phenomena, which will be explained below. In order to recover part of the remaining oil from wells (called production wells), it is used the way that one injects a water into another wells (injection wells), which are located around the reservoir, so that the water pushes the oil toward the production wells, and then the oil can be recovered. In this process, two immiscible fluids, water and oil, can be regarded as separated by a sharp interface during the penetration of water into oil. By laboratory studies, it is already known that the interface is unstable; small perturbations in the interface grow up (see [2] or Fig. 18). This phenomenon is called the *fingering instability*. When the area of water reaches the production wells, pockets of by-passed oil are created, and water is produced from production wells, which is economically unfavorable.

Similar phenomenon is observed in the Hele-Shaw cell involving flow in thin gaps [14], and also observed in the flow caused by Rayleigh-Taylor instability [16]. In the former, the interface between two immiscible fluids becomes unstable and forms fingers, when a less viscous fluid moves slowly between two parallel horizontal plates separated by a thin gap, in which a more viscous fluid is filled. In the latter, the interface also exhibits a fingering pattern, when a lighter fluid fails to support a heavier fluid against the action of gravity.

Especially, to analyze the oil recovery process, mathematical models have been proposed and studied from numerical points of view, where the capillary pressure between water and oil is ignored ([8], [5], [6], [18] and the references therein). In particular, the Buckley-Leverett equations, which consist of the one hyperbolic equation and the two elliptic equations, are well known in the petroleum literature. Glimm et al [8] show some numerical simulations for these equations, and indicate the occurrence of the fingering instability. Similar simulations are done in [5], [6] and [18], where the interface with a

small perturbation grows fingers. From the analytical points of view, Chorin [2] proves under some special initial and boundary conditions that the interface is linearly unstable if $\mu = \mu_o/\mu_w > 3$ and is linearly stable if $\mu < 3$, where μ_o and μ_w are the viscosities of oil and water, respectively.

When water is injected with low pressure, it is known that the capillary pressure plays an important role to determine the behavior of the interface. So, we can not always ignore the capillary pressure. This situation can be easily modelled by the equations by adding the effect of the capillary pressure to the Buckley-Leverett equations. Dahle et al in [18] introduce Petrov-Galerkin subdomain methods for the one dimensional problem and show some numerical simulations with the low capillary pressure. However, the effect of the capillary pressure to the interface is not discussed there.

Motivated the above results, we consider the behavior of the interface when the capillary pressure becomes high. For this investigation, we first consider the one dimensional problem from numerical and analytical points of view. We carry on the numerical simulations in two cases where the capillary pressure is zero and is high. The numerical simulations for large values of μ (more precisely, see Remark 9) give us the following suggestions:

1a) The acceleration of the interface is positive when the capillary pressure is zero;
1b) The acceleration of the interface is negative when the capillary pressure is sufficiently large;
1c) The interface fails to move and may stop at some point when the acceleration is negative.

We will prove 1a) and 1c) for an injection with negative pressure. However, 1b) has not been able to be proved.

Next, we consider the two dimensional problem. We numerically show the following:

2a) The fingering instability occurs when the capillary pressure is zero;
2b) The fingering instability disappears when the capillary pressure is sufficiently large;
2c) The interface may stop and there may exist a steady state solution when the negative pressure is given at the injection well.

The justification of these numerical results has not been yet done.

The outline of this paper is as follows. In the next section, we present the basic equations, and introduce a one dimensional problem of these equations, which is treated in Section 3. In Subsection 3.1, we propose a numerical difference scheme and prove the boundedness and the monotonicity

preserving of numerical solutions. In Subsection 3.2, using some interface equation, we apply the idea used in [11] and [13] to constructing an interface-tracking difference scheme, and prove the the boundedness and the monotonicity preserving of solutions. We demonstrate some numerical simulations in Subsection 3.3, and show 1a)-1c). We justify 1a) and 1c) in Subsections 3.4 and 3.5, respectively. In Section 4, the two dimensional problem is discussed from points of numerical simulations.

ACKNOWLEDGMENTS. The author would like to express his gratitude to Professor Masayasu Mimura of Hiroshima University for his inspiring suggestion and continued encouragement. He also would like to thank Professor Kenji Tomoeda of Osaka Institute of Technology for his help to read the manuscript and to suggest a number of improvements, and to Professor Toshitaka Nagai of Kyushu Institute of Technology for his stimulating discussion. The numerical simulations in this paper were made on a computer FX/1 in Department of Mathematics, Hiroshima University and workstations Sun 4/490 and Sun 4/1 in Fukuoka University of Education.

2. The basic equations

In this section, we introduce the basic equations to analyze the oil recovery process. For this purpose, we write water and oil as *fluid w* and *fluid o*, respectively. Let the saturation $s_i(x, t)$ be the fractional amount of fluid i $(i = w, o)$ at point x and time t. We denote by $v_i(x, t)$ and $p_i(x, t)$ the velocity and the pressure of fluid i, respectively. Then the equations for the oil reservoir problem are

$$s_w + s_o = 1, \tag{2.1}$$

$$-\nabla \cdot \rho_i v_i = \frac{\partial}{\partial t}(n\rho_i s_i), \qquad i = w, o, \tag{2.2}$$

$$v_i = -\frac{Kk_i}{\mu_i}(\nabla p_i - \rho_i g), \qquad i = w, o, \tag{2.3}$$

$$p_o - p_w = p_c \tag{2.4}$$

(see [1] and [15]). Here, ρ_i and μ_i are the density and viscosity of fluid i $(i = w, o)$, n and K are the porosity and absolute permeability of the medium. g is the gravity constant. $k_w = k_w(s_o)$ and $k_o = k_o(s_w)$ are the relative permeabilities of fluid w and o, respectively, and $p_c = p_c(s_w)$ is the capillary pressure between two fluids. The forms of these functions are given by experiments (see Remark 1).

The equation (2.2) expresses the conservation of fluid i, and the equation (2.3) is Darcy's law, which means that the flow of i is proportional to the gradient of its pressure. The last equation (2.4) is the balance law of pressures.

For simplicity, we assume that ρ_i, μ_i $(i = w, o)$, n and K are uniformly constants with respect to x and t, and that $g = 0$. By putting $s = s_w$, $v = v_w + v_o$ and $p = p_w$, the equations (2.1)–(2.4) are rewritten as follows.

$$\frac{\partial}{\partial t}s + \nabla \cdot [vf] - \varepsilon \nabla \cdot [f\phi \nabla s] = 0, \tag{2.5}$$

$$\nabla \cdot v = 0, \tag{2.6}$$

$$v = -[\lambda \nabla p - \varepsilon \phi \nabla s], \tag{2.7}$$

where

$$f = f(s) = \frac{k_w(s)}{\lambda(s)}, \quad \lambda = \lambda(s) = k_w(s) + \frac{k_o(s)}{\mu}, \quad \mu = \frac{\mu_o}{\mu_w},$$

$$\phi(s) = -\frac{k_o(s)}{\varepsilon\mu}p_c'(s) \quad \text{and} \quad \varepsilon = \max_{0 \le s \le 1} |p_c'(s)|.$$

Here (2.6) follows from (2.1) and (2.2), and (2.7) is obtained from (2.3) by replacing $\frac{K}{\mu_w}x$ by x. (2.5) is also obtained from (2.7), (2.2) and (2.3) by replacing $\frac{K}{n\mu_w}t$ by t.

REMARK 1. It is observed by experiments [3] that p_c is a monotone decreasing function. For an example of explicit forms of k_w and k_o, we take these as

$$k_w(s) = s^2 \quad \text{and} \quad k_o(s) = (1 - s)^2, \tag{2.8}$$

so that

$$\lambda(s) = s^2 + \frac{(1 - s)^2}{\mu} \quad \text{and} \quad f(s) = \frac{s^2}{\lambda(s)}. \tag{2.9}$$

Taking the above information on p_c, k_o, f and λ into considerations, we can impose Conditions A, B and C on ϕ, f and λ, respectively.

CONDITION A. ϕ is a continuous function defined on $[0, 1]$ and $\phi(s) > 0$ holds for almost all $s \in [0, 1]$.

CONDITION B. $f = f(s) \in C^2[0, 1]$ is a monotone increasing function such

that

$$f'(0) = f'(1) = 0, \quad f(0) = 0 \quad \text{and} \quad f(s) > 0 \ (0 < s \leq 1), \tag{2.10}$$

and there exists only one constant $s^* \in (0, 1)$ satisfying

$$\frac{f(s^*)}{s^*} = f'(s^*). \tag{2.11}$$

For this constant s^*,

$$f'' < 0 \quad \text{on} \quad [s^*, 1] \tag{2.12}$$

holds.

CONDITION C. $\lambda = \lambda(s) \in C^0[0, 1]$ is a positive function satisfying

$$\lambda(s) \geq \lambda(s^*) \quad \text{on} \quad [s^*, 1], \tag{2.13}$$

where s^* is the constant in Condition B.

We note that when λ and f satisfy (2.9), Condition B holds with $s^* = 1/\sqrt{1+\mu}$. When $\varepsilon = 0$, (2.5)–(2.7) are called the Buckley-Leverett equations [1].

We consider the one dimensional problem for (2.5)–(2.7) on $x \in I \equiv (0, 1)$ and $t > 0$ under the boundary conditions

$$s(0, t) = 1, \quad p(0, t) = p^* \qquad \text{on} \quad t > 0, \tag{2.14}$$

$$s(1, t) = 0, \quad p(1, t) = 0 \qquad \text{on} \quad t > 0, \tag{2.15}$$

with the initial condition

$$s(x, 0) = s^0(x) \qquad \text{on} \quad x \in I, \tag{2.16}$$

where s^0 satisfies $0 \leq s^0 \leq 1$. (2.14) and (2.15) describe the injection of water with the pressure p^* at $x = 0$ and the production of oil at $x = 1$, respectively. In this problem, (2.6) implies that $v(x, t)$ is independent of x. Then from (2.7), we have

$$v \int_0^1 \frac{dx}{\lambda(s)} + \varepsilon \int_0^1 \frac{\phi(s)}{\lambda(s)} s_x \, dx = -\int_0^1 p_x \, dx.$$

Using this equation, we can rewrite the equations (2.5)–(2.7), and boundary conditions (2.14)–(2.15) as follows:

$$s_t + v f(s)_x - \varepsilon (d(s) s_x)_x = 0 \quad \text{on} \quad x \in I, \ t > 0, \tag{2.17}$$

$$v = (p^* - c\varepsilon) \left(\int_0^1 \frac{dx}{\lambda(s)} \right)^{-1} \quad \text{on} \quad t > 0, \tag{2.18}$$

$$s(0, t) = 1 \quad \text{and} \quad s(1, t) = 0 \quad \text{on} \quad t > 0, \tag{2.19}$$

where

$$c = \int_0^1 \frac{\phi(\sigma)}{\lambda(\sigma)} d\sigma \tag{2.20}$$

is some constant and $d(s) = f(s)\phi(s)$. The unknown variables are $s(x, t)$ and $v(t)$, where $p(x, t)$ is eliminated.

REMARK 2. From (2.17) and (2.18), we have

$$\frac{1}{\varepsilon} s_t + \left(\frac{p^*}{\varepsilon} - c \right) \left(\int_0^1 \frac{dx}{\lambda(s)} \right)^{-1} f(s)_x - (d(s)s_x)_x = 0.$$

Replacing εt by t, we find that the parameters p^* and ε appear in the form of p^*/ε. Therefore, changing the value of ε means that the value of the pressure p^*, which is given at the injection well, varies.

When $\varepsilon > 0$, because $d(0) = d(1) = 0$, the diffusion term $\varepsilon(d(s)s_x)_x$ of (2.17) degenerates at $s = 0$ and $s = 1$, so that, there possibly appear interfaces between $s = 0$ and $s > 0$ and between $s = 1$ and $s < 1$. On the other hand, when $\varepsilon = 0$, (2.17) is a nonlinear hyperbolic equation, and a shock-interface between $s = 0$ and $s > 0$ exists (see Subsection 3.4). In both cases, the interface between $s = 0$ and $s > 0$ appears, and, in oil-reservoir problems, this interface separates an area where water penetrates from an oil-region.

When $\varepsilon > 0$, the existence and uniqueness of the solution of (2.16)–(2.19) are proved by Mochizuki and Suzuki [12]. However, the behavior of the interface is not studied. For this reason, we rely on numerical methods to understand qualitative and quantitative behaviors. In the following section, we present two numerical methods. One is for (2.16)–(2.19) and the other is for the interface equation (see (3.16)) derived from (2.16)–(2.19).

3. One dimensional problem

3.1. The difference scheme for numerical solutions

In this subsection, we introduce a finite difference scheme for the one dimensional problem (2.17)–(2.18) under the boundary and the initial conditions (2.19) and (2.16), and prove the boundedness and the monotonicity preserving of the numerical solutions.

Let J be a positive integer, and put $\Delta x = 1/J$. We denote by s_j^n and v^n the numerical approximations to $s(x_j, t_n)$ and $v(t_n)$, respectively, where $x_j = j\Delta x$ $(j = 0, 1, \ldots, J)$ and $\{t_n\}_{n=0,1,\ldots}$ is an increasing sequence, which will be

determined later. Our difference scheme is written in the following form: For all $n \geq 0$,

$$\frac{s_j^{n+1} - s_j^n}{\Delta t_n} + v^n \frac{f(s_j^n) - f(s_{j-1}^n)}{\Delta x} - \varepsilon D_h s_j^n = 0 \quad (1 \leq j \leq J-1), \quad \text{if } v^n \geq 0, \tag{3.1}$$

$$\frac{s_j^{n+1} - s_j^n}{\Delta t_n} + v^n \frac{f(s_{j+1}^n) - f(s_j^n)}{\Delta x} - \varepsilon D_h s_j^n = 0 \quad (1 \leq j \leq J-1), \quad \text{if } v^n < 0, \tag{3.2}$$

$$v^n = (p^* - c\varepsilon)\left[\Delta x\left(\frac{1}{2\lambda(s_0^n)} + \sum_{j=1}^{J-1} \frac{1}{\lambda(s_j^n)} + \frac{1}{2\lambda(s_J^n)}\right)\right]^{-1}, \tag{3.3}$$

$$s_0^n = 1 \quad \text{and} \quad s_J^n = 0, \tag{3.4}$$

$$s_j^0 = s^0(x_j) \quad (0 \leq j \leq J), \tag{3.5}$$

where

$$0 \leq s^0 \leq 1 \quad \text{on } [0, 1], \tag{3.6}$$

$$D_h s_j^n = \frac{1}{\Delta x^2}\left\{d\left(\frac{s_{j+1}^n + s_j^n}{2}\right)(s_{j+1}^n - s_j^n) - d\left(\frac{s_j^n + s_{j-1}^n}{2}\right)(s_j^n - s_{j-1}^n)\right\} \tag{3.7}$$

and $d(s) = f(s)\phi(s)$. Here, we construct the difference schemes (3.1) and (3.2) by applying the idea of Engquist-Osher's one-sided scheme [4] to the convection term $vf(s)_x$ of (2.17). The equation (3.3) is obtained from (2.18) by the numerical integration.

Taking $t_0 = 0$, we inductively compute the numerical solutions $\{s_j^n\}_{j=0,1,\ldots,J}$ and v^n at $t = t_n$ by the scheme (3.1)–(3.5), where $\Delta t_n = t_{n+1} - t_n$ is the variable time step and satisfies

$$\Delta t_n \leq \frac{\Delta x^2}{\Delta x |v^n| \, \|f'\| + 2\varepsilon \, \|d\|}, \tag{3.8}$$

where $\| \cdot \| = \| \cdot \|_{L^\infty(0,1)}$.

THEOREM 1. *Under Conditions A, B and C, let* (3.8) *be satisfied for all* $n \geq 0$. *Then, it follows that*

$$0 \leq s_j^n \leq 1 \ (0 \leq j \leq J) \quad \textit{for all } n \geq 0. \tag{3.9}$$

Moreover, if the initial function $s^0(x)$ *decreases monotonously,*

$$s_j^n \geq s_{j+1}^n \ (0 \leq j \leq J-1) \quad \textit{for all } n \geq 0 \tag{3.10}$$

holds.

THEOREM 2. *Let the assumptions of Theorem* 1 *be satisfied. Then, for*

each Δx, there exists a positive number δ such that

$$\frac{\Delta x^2}{\Delta x|v^n|\,\|f'\| + 2\varepsilon\|d\|} \geq \delta \quad \text{for all } n \geq 0. \tag{3.11}$$

REMARK 3. For some constant α satisfying $0 < \alpha \leq 1$, we take

$$\Delta t_n = \alpha \frac{\Delta x^2}{\Delta x|v^n|\,\|f'\| + 2\varepsilon\|d\|}.$$

Then $\lim_{n\to\infty} t_n = \infty$ follows from (3.11).

We will state the proofs of Theorems 1 and 2 in Section 5.

3.2. The difference scheme for numerical interfaces

In this subsection, we construct the numerical approximations to track the interface of the solution. We define the interface $\ell(t)$ of the solution s of (2.17)–(2.19) by

$$\ell(t) = \inf\{\xi;\, s(x, t) = 0 \quad \text{on} \quad \xi < x < 1\}.$$

When $\varepsilon = 0$, the solution consists of a shock wave connecting $s = 0$ and $s = s^*$, where s^* is the constant defined by (2.11) (see Subsections 3.4 and 3.5). Then it is natural to define a numerical interface at $t = t_n$ by

$$\ell_n = \min\left\{\xi;\, s_h^n(x) \leq \frac{s^*}{2} \quad \text{on} \quad \xi < x < 1\right\}, \tag{3.12}$$

where $s_h^n(x)$ is a piecewise linear function interpolating $\{(x_j, s_j^n)\}_{j=0,1,\ldots,J}$ computed by (3.1)–(3.5).

When $\varepsilon > 0$, the shock wave disappears by the effect of the diffusion term $\varepsilon(d(s)s_x)_x$ of (2.17), and the solution may be continuous on $0 < x < 1$. From this, (3.12) is not available to determine the numerical interfaces. Therefore, it is necessary to find an interface equation, from which numerical interfaces can be obtained. For this purpose, we introduce

CONDITION D. There exist constants $p > 0$ and $m > 1$ such that

$$\lim_{s\to 0} \frac{f(s)}{s^p} = c_1 > 0 \quad \text{and} \quad \lim_{s\to 0} \frac{d(s)}{s^{m-1}} = c_2 > 0, \tag{3.13}$$

$$p \geq \frac{m+1}{2}. \tag{3.14}$$

Under Condition D, we can formally rewrite (2.17) as

$$s_t + c_1 v(s^p)_x - \frac{c_2 \varepsilon}{m}(s^m)_{xx} = 0 \qquad \text{for sufficiently small } s. \tag{3.15}$$

B. H. Gilding [7] proves that the interface $\ell(t)$ of the solution of (3.15) with (3.14) satisfies

$$\ell'(t) = -\frac{c_2 \varepsilon}{m-1}(s^{m-1})_x(\ell(t) - 0, t). \tag{3.16}$$

Using (3.16), we construct the numerical interfaces. Although we have not proved that whether (3.16) is valid for (2.16)–(2.19) or not, our numerical simulations suggest us that (3.16) is plausible.

From the above consideration, we apply the idea used in [11] and [13] to constructing the difference scheme, which tracks the interface. Our discretization of (2.16)–(2.19) and (3.16) is as follows: For all $n \geq 0$,

$$\ell_{n+1} = \ell_n + \Delta t_n \frac{\varepsilon c_2}{m-1} \frac{(s^n_{L_n})^{m-1}}{h_n}, \tag{3.17}$$

$$\frac{s_j^{n+1} - s_j^n}{\Delta t_n} + v^n \frac{f(s_j^n) - f(s_{j-1}^n)}{\Delta x} - \varepsilon D_h s_j^n = 0 \quad (1 \leq j \leq L_n - 1), \quad \text{if } v^n \geq 0, \tag{3.18}$$

$$\frac{s_j^{n+1} - s_j^n}{\Delta t_n} + v^n \frac{f(s_{j+1}^n) - f(s_j^n)}{\Delta x} - \varepsilon D_h s_j^n = 0 \quad (1 \leq j \leq L_n - 1), \quad \text{if } v^n < 0, \tag{3.19}$$

$$\frac{s_{L_n}^{n+1} - s_{L_n}^n}{\Delta t_n} + v^n \frac{f(s_{L_n}^n) - f(s_{L_n-1}^n)}{\Delta x} - \varepsilon D_h' s_{L_n}^n = 0 \quad \text{if } v^n \geq 0, \tag{3.20}$$

$$\frac{s_{L_n}^{n+1} - s_{L_n}^n}{\Delta t_n} + v^n \frac{-f(s_{L_n}^n)}{h_n} - \varepsilon D_h' s_{L_n}^n = 0 \quad \text{if } v^n < 0, \tag{3.21}$$

$$s_j^{n+1} = s_{L_{n+1}-1}^{n+1} \frac{\ell_{n+1} - j\Delta x}{\ell_{n+1} - L_{n+1}\Delta x} \quad (L_n + 1 \leq j \leq L_{n+1}), \tag{3.22}$$

$$s_j^{n+1} = 0 \quad (L_{n+1} + 1 \leq j \leq J), \tag{3.23}$$

$$v^n = (p^* - c\varepsilon)\left[\frac{\Delta x}{2\lambda(s_0^n)} + \sum_{j=1}^{L_n - 1} \frac{\Delta x}{\lambda(s_j^n)} + \frac{h_n}{2\lambda(s_{L_n}^n)} + \frac{1 - \ell_n}{\lambda(0)}\right]^{-1}, \tag{3.24}$$

$$s_0^n = 1 \quad \text{and} \quad s_J^n = 0, \tag{3.25}$$

$$s_j^0 = s^0(x_j) \quad (0 \leq j \leq J), \tag{3.26}$$

$$\ell_0 = \ell^0, \tag{3.27}$$

where $h_n = \ell_n - L_n \Delta x$,

$$L_n = \max\{j \in \mathbf{Z}; j\Delta x < \ell_n\}, \tag{3.28}$$

$$D_h' s_L^n = \frac{2}{\Delta x + h}\left\{d\left(\frac{s_L^n}{2}\right)\frac{-s_L^n}{h} - d\left(\frac{s_L^n + s_{L-1}^n}{2}\right)\frac{s_L^n - s_{L-1}^n}{\Delta x}\right\}, \tag{3.29}$$

the difference operator D_h is given by (3.7) and $\ell^0 \in (0, 1)$ is a constant satisfying

$$0 < s^0(x) \leq 1 \quad \text{on } [0, \ell^0) \quad \text{and} \quad s^0(x) = 0 \quad \text{on } [\ell^0, 1]. \tag{3.30}$$

For $j = 0, 1, \ldots, L_n - 1$, the equations (3.18) and (3.19) are the same ones as (3.1) and (3.2), respectively. Since $0 < h_n < \Delta x$ holds in general, we use (3.20), (3.21) and (3.29) instead of (3.1), (3.2) and (3.7) at $j = L_n$, respectively. For the same reason, we use (3.24) instead of (3.3). We also interpolate $(x_{L_n}, s_{L_n}^{n+1})$ and $(\ell_{n+1}, 0)$ by (3.22) to determine numerical solutions s_j^{n+1} $(L_n + 1 \leq j \leq L_{n+1})$, which cannot be computed by (3.18)–(3.21) and (3.23).

REMARK 4. In the case where k_o, λ and f are given by (2.8)–(2.9) and $p_c'(s)$ is negative and bounded on $[0, 1]$, Condition D is satisfied with $p = 2$ and $m = 3$. Since (3.28) can not be defined for $\ell^0 = 0$, we assume that ℓ^0 is positive.

We determine the time step Δt_n satisfying (3.8) and

$$\Delta t_n \leq \frac{\tau_1 \tau_2}{\tau_1 + \tau_2}, \tag{3.31}$$

$$\ell_n + \Delta t_n \frac{\varepsilon c_2}{m-1}\frac{(s_L^n)^{m-1}}{h} \leq 1, \tag{3.32}$$

$$\Delta t_n \frac{\varepsilon c_2}{m-1}\frac{(s_L^n)^{m-1}}{h} \leq \Delta x, \tag{3.33}$$

where $L = L_n$, $h = h_n$ and

$$\tau_1 = \frac{\Delta x s_L^n}{|v^n| f'(s_L^n)}, \quad \tau_2 = \frac{h\Delta x(h + \Delta x)}{2\varepsilon\left(d\left(\frac{s_L^n}{2}\right)\Delta x + d\left(\frac{s_L^n + s_{L-1}^n}{2}\right)h\right)}. \tag{3.34}$$

Then, we obtain the result similar to that of Theorem 1.

THEOREM 3. *Under Conditions A, B, C and D, let* (3.8) *and* (3.31)–(3.33) *be satisfied for all* $n \geq 0$. *Then the conclusions of Theorem* 1 *hold.*

The proof of Theorem 3 will be stated in Section 5.

3.3. Numerical simulations

In this subsection, we carry on some numerical simulations and show 1a)–1c) stated in Section 1. Let the functions $k_o(s)$, $\lambda(s)$ and $f(s)$ be given by (2.8)–(2.9), and $p_c(s) = \varepsilon(1 - s)$. To see the behavior of interface, we use the scheme (3.1)–(3.6) and (3.12) if $\varepsilon = 0$, and the scheme (3.17)–(3.27) if $\varepsilon > 0$.

At first, let us consider the case of $\varepsilon = 0$. The initial function takes $s^0 \equiv 0$, which implies that the medium is filled by oil at initial time. Fig. 1 shows the numerical solution s with $\mu = 20$. The numerical interface is shown in Fig. 2, which suggests us that the interface $\ell(t)$ moves with gradually increasing speed. Let us change the value of μ. Figs. 3 and 4 show the numerical solution and the interface, respectively, with $\mu = 0.5$, and the speed of $\ell(t)$ seems to decrease. These results suggest us that the acceleration of the interface depends on μ, and that there exists a constant μ^* such that the speed of $\ell(t)$ increases for $\mu > \mu^*$, while it decreases for $\mu < \mu^*$, which leads to 1a). We will show in the following subsection that 1a) holds.

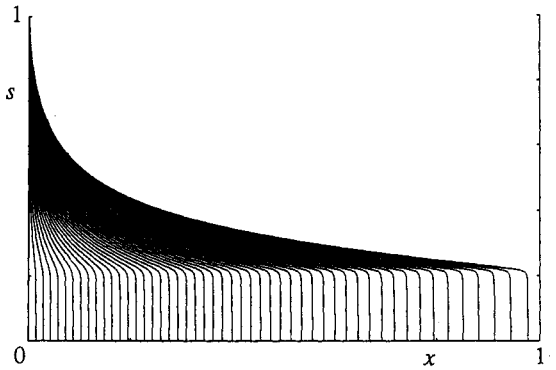

Fig. 1 Numerical solution of (2.17)–(2.19) with $\varepsilon = 0$, $\mu = 20$, $p^* = 1$ and $\Delta x = 0.001$ at $t = 0, 0.1, 0.2, \ldots, 4.9$.

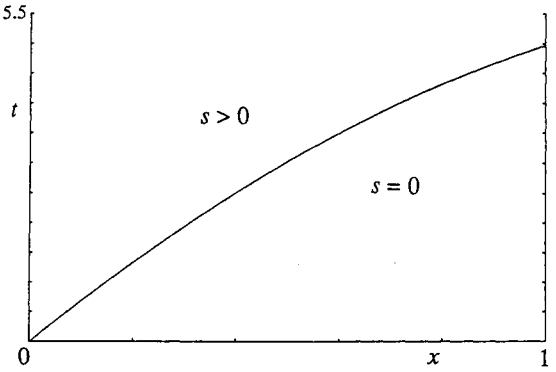

Fig. 2 Interface of numerical solution in Fig. 1.

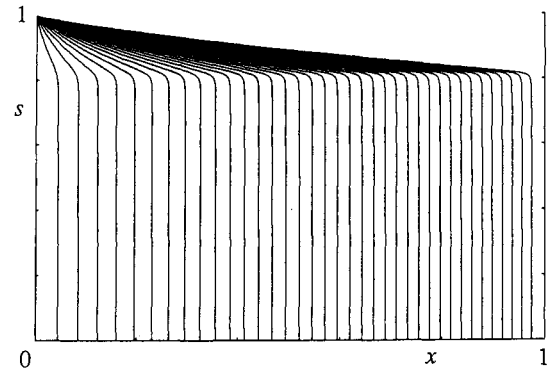

Fig. 3 Numerical solution of (2.17)–(2.19) with $\varepsilon = 0$, $\mu = 0.5$, $p^* = 1$ and $\Delta x = 0.001$ at $t = 0, 0.02, 0.04, \ldots, 0.74$.

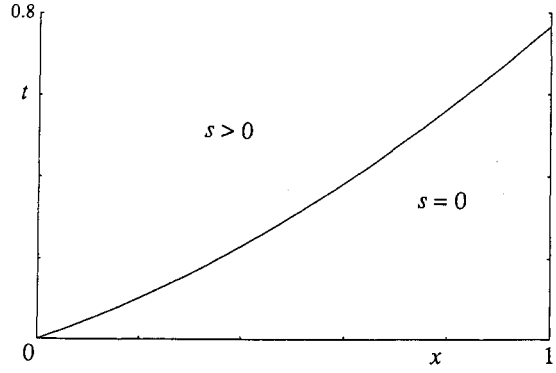

Fig. 4 Interface of numerical solution in Fig. 3.

Next, we try to compute when $\varepsilon > 0$. In this case we take $\mu = 20$ and

$$s^0(x) = 1 \quad \text{if } x < 0.05, \quad s^0(x) = 0 \text{ otherwise.} \tag{3.35}$$

Figs. 5 and 6 demonstrate the numerical solution and interface with $\varepsilon = 0.01$, respectively. Since ε is small, the acceleration is still positive, which is the same property as stated in the case of $\varepsilon = 0$. Let $\varepsilon = 1$. Figs. 7 and 8 show the numerical solution and interface, respectively. In this case, the acceleration of the interface becomes small as compared with the case of $\varepsilon = 0.01$. We next try the numerical computations for $\varepsilon = 100$ in Figs. 9 and 10, which show that the acceleration is negative. This means 1b). From the above considerations, one expects that the acceleration becomes negative for large ε. However, we can not prove it.

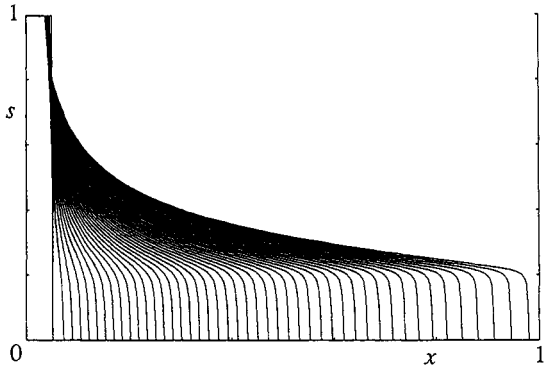

Fig. 5 Numerical solution of (2.17)–(2.19) with $\varepsilon = 0.01$, $\mu = 20$, $p^* = 1$ and $\Delta x = 0.001$ at $t = 0, 0.1, 0.2, \ldots, 4.4$.

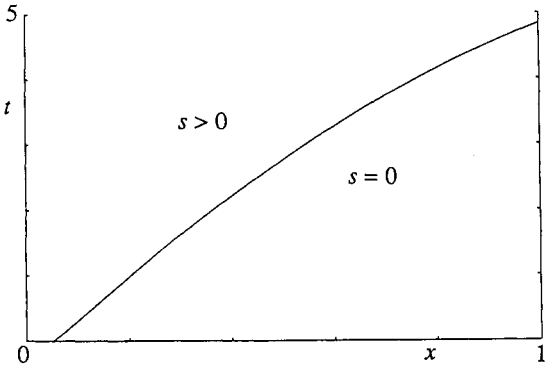

Fig. 6 Interface of numerical solution in Fig. 5.

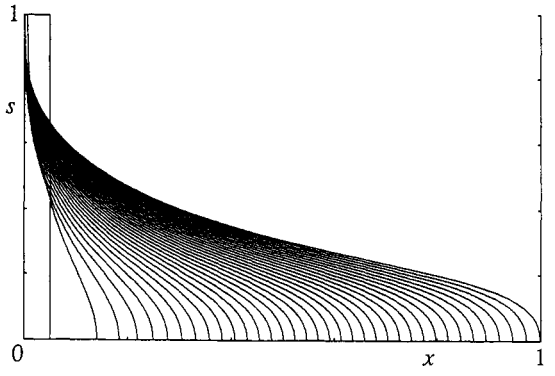

Fig. 7 Numerical solution of (2.17)–(2.19) with $\varepsilon = 1$, $\mu = 20$, $p^* = 1$ and $\Delta x = 0.001$ at $t = 0, 0.1, 0.2, \ldots, 3.5$.

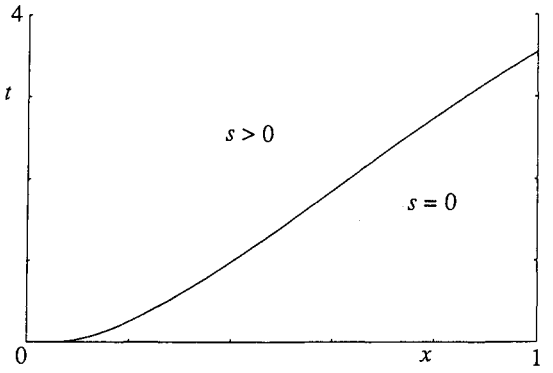

Fig. 8 Interface of numerical solution in Fig. 7.

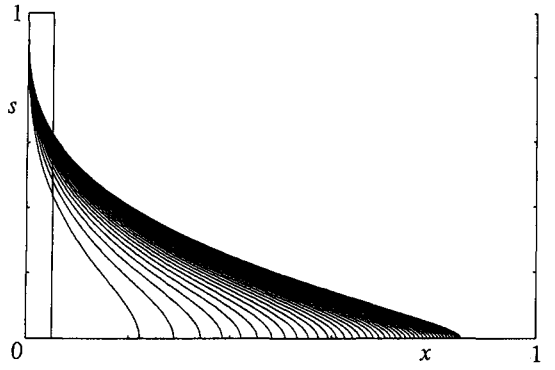

Fig. 9 Numerical solution of (2.17)–(2.19) with $\varepsilon = 100$, $\mu = 20$, $p^* = 1$ and $\Delta x = 0.001$ at $t = 0, 0.005, 0.01, \ldots, 0.2$.

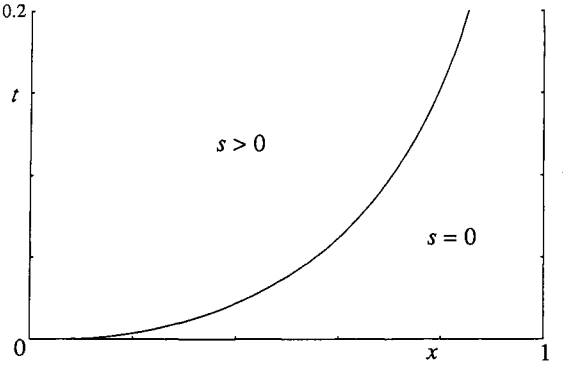

Fig. 10 Interface of numerical solution in Fig. 9.

Finally, we consider 1c). The graphs of the numerical interface suggest us that the value of the acceleration becomes negative as ε becomes larger. Therefore, for large ε, it seems that the interface fails to move. If the interface stops, we may expect that a steady state solution exists. This motivates us to study the existence of steady state solutions, which will be stated in Subsection 3.5. We give a brief summary of the result. In the case of $p^* > 0$, there is no steady state solution, which means that the interface never stop. Therefore, 1c) is not true for $p^* > 0$ and the interface reaches to $x = 1$. On the other hand, if $p^* \leq 0$, the steady state solution exists and the interface will stop. That is, 1c) holds for $p^* \leq 0$ (see Figs. 11 and 12).

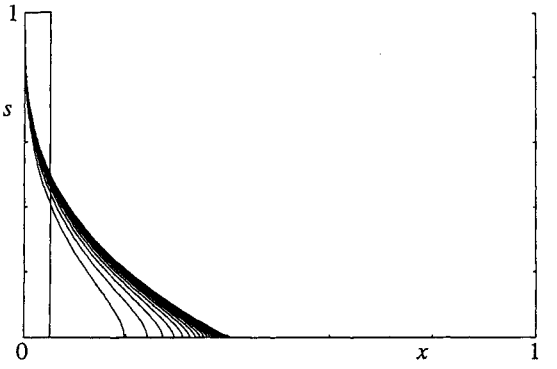

Fig. 11 Numerical solution of (2.17)–(2.19) with $\varepsilon = 100$, $\mu = 20$, $p^* = -50$ and $\Delta x = 0.001$ at $t = 0, 0.005, 0.01, \ldots, 0.5$.

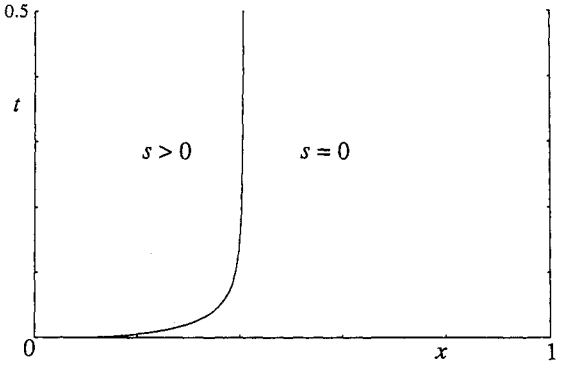

Fig. 12 Interface of numerical solution in Fig. 11.

3.4 The behavior of interfaces when $\varepsilon = 0$

In this subsection, we show the behavior of the interface for the solution of

$$s_t + v f(s)_x = 0, \tag{3.36}$$

$$v = p^* \left[\int_0^1 \frac{dx}{\lambda(s)} \right]^{-1}, \tag{3.37}$$

under the boundary condition (2.19) and the initial condition

$$s(x, 0) = s^0(x). \tag{3.38}$$

The equations (3.36)–(3.37) are called the Buckley-Leverett equations. Throughout this subsection, we assume $p^* > 0$. For this problem, taking $s^0 \equiv 0$, we investigate the behavior of the interface of the solution to (3.36)–(3.38).

The equation (3.36) is a single conservation law with the nonlinear function $f(s)$. It is well known that (3.36) has discontinuous solutions, which are called shock waves. When v is independent of t, this discontinuous solution consists of the rarefaction wave connecting constant states 1 and s^* and the shock wave by which constant states s^* and 0 are separated (see [10]). Here, s^* is the constant defined by (2.11). Taking the property of this solution into considerations, we obtain the following theorem for solutions of (3.36)–(3.38).

THEOREM 4. *Assume $s^0 \equiv 0$. Under Conditions A, B and C, the pair of functions $s(x, t)$ and $v(t)$ defined by*

$$s(x, t) = \begin{cases} a^{-1}(x/V(t)) & \text{if } 0 \le x \le \ell(t), \\ 0 & \text{if } \ell(t) < x \le 1, \end{cases} \tag{3.39}$$

$$v(t) = 1/\sqrt{2\frac{A}{p^*}t + \left(\frac{B}{p^*}\right)^2} \tag{3.40}$$

is a weak solution of (3.36)–(3.38) *and* (2.19), *where a^{-1} is the inverse function of $a(s) \equiv f'(s)$ $(s^* \le s \le 1)$,*

$$V(t) = \int_0^t v(\tau)\, d\tau, \tag{3.41}$$

$$\ell(t) = a(s^*) V(t), \tag{3.42}$$

$$A = \int_{s^*}^1 \frac{-a'(\sigma)}{\lambda(\sigma)}\, d\sigma - \frac{a(s^*)}{\lambda(0)} \quad \text{and} \quad B = \frac{1}{\lambda(0)}. \tag{3.43}$$

REMARK 5. By (2.12) a is a strictly monotone decreasing function on

$[s^*, 1]$. Therefore, a^{-1} exists, and the function s is well-defined.

REMARK 6. The function $s(x, t)$ defined by (3.39) is discontinuous on $x = \ell(t)$, and $s(x, t) = 0$ for $x \in (\ell(t), 1]$. It implies that the function $\ell(t)$ becomes the interface of s.

Before showing the proof of the theorem, we state the definition of the weak solution of (3.36)–(3.38) and (2.19).

DEFINITION 1. A pair of functions $s(x, t)$ and $v(t)$ is a weak solution of (3.36)–(3.38) and (2.19) if

i) s is a bounded measurable function and v is continuous;
ii) s and v satisfy (3.37), (3.38) and (2.19);
iii) For an arbitrary number $T > 0$ and for any test function $\varphi \in C^1$ with supp $\varphi \subset (0, 1) \times [0, T)$,

$$\int_0^T \int_0^1 (s\varphi_t + vf(s)\varphi_x)\, dx\, dt + \int_0^1 s(x, 0)\varphi(x, 0)\, dx = 0 \tag{3.44}$$

holds.

REMARK 7. We do not know the uniqueness of the weak solution defined above.

PROOF OF THEOREM 4. It is easy to verify that s and v satisfy i) in Definition 1, (3.38) and (2.19). First, let us show that s and v satisfy (3.37). From (3.39), we have

$$\begin{aligned} \int_0^1 \frac{dx}{\lambda(s)} &= \int_0^{\ell(t)} \frac{dx}{\lambda(a^{-1}(x/V(t)))} + \int_{\ell(t)}^1 \frac{dx}{\lambda(0)} \\ &= V(t) \int_{s^*}^1 \frac{-a'(\sigma)}{\lambda(\sigma)}\, d\sigma + \frac{1 - a(s^*)V(t)}{\lambda(0)} \\ &= AV(t) + B, \end{aligned} \tag{3.45}$$

where $\sigma = a^{-1}(x/V(t))$. On the other hand, since

$$\begin{aligned} V(t) &= \int_0^t 1 \Big/ \sqrt{2\frac{A}{p^*}t + \left(\frac{B}{p^*}\right)^2}\, d\tau \\ &= \frac{p^*}{A}\sqrt{2\frac{A}{p^*}t + \left(\frac{B}{p^*}\right)^2} - \frac{B}{A} \\ &= \frac{1}{A}\left\{\frac{p^*}{v(t)} - B\right\} \end{aligned}$$

holds by (3.40) and (3.41), we obtain

$$v(t)\{AV(t)+B\}=p^*. \tag{3.46}$$

From (3.45) and (3.46), (3.37) holds, and ii) in Definition 1 is satisfied.

Next, we show iii). It is easily shown that s satisfies (3.36) in the classical sense on $(0, \ell(t))\cup(\ell(t), 1)$. To prove that s satisfies (3.44), it suffices to show that the Rankine-Hugoniot jump condition (see (3.48)) is satisfied at points where s is discontinuous. Since it follows from (3.42) and (3.39) that $s(\ell(t)+0, t)=0$ and $s(\ell(t)-0, t)=s^*$, we have

$$\frac{v(t)f(s(\ell(t)+0, t))-v(t)f(s(\ell(t)-0, t))}{s(\ell(t)+0, t)-s(\ell(t)-0, t)}=v(t)f(s^*)/s^*. \tag{3.47}$$

Hence, we have from (2.11), (3.41), (3.42) and (3.47)

$$\ell'(t)=f'(s^*)v(t)=\frac{v(t)f(s(\ell(t)+0, t))-v(t)f(s(\ell(t)-0, t))}{s(\ell(t)+0, t)-s(\ell(t)-0, t)}, \tag{3.48}$$

which is the Rankine-Hugoniot jump condition (see [9], [17], for example). Thus, the proof is complete.

Next, we show the behavior of the interface of the solution s in Theorem 4.

THEOREM 5. *Let the assumptions of Theorem* 4 *be satisfied. For the interface* $\ell(t)$ *in Theorem* 4, *it follows that*

$$\ell'(t)>0 \quad \textit{on} \quad 0<t<T_b \tag{3.49}$$

for some constant $T_b>0$ *satisfying* $\ell(T_b)=1$. *Moreover, if* $\lambda(s^*)>\lambda(0)$, *then*

$$\ell''(t)>0 \quad \textit{on} \quad 0<t<T_b \tag{3.50}$$

holds.

COROLLARY. *In the case of* (2.8)–(2.9), (3.50) *holds for* $\mu>3$.

REMARK 8. The constant T_b is called the breakthrough time [8].

PROOF OF THEOREM 5. Let us prove the existence of the constant $T_b>0$ satisfying

$$\ell(T_b)=a(s^*)V(T_b)=1. \tag{3.51}$$

When $A>0$, it follows from (3.40) that

$$v(t)\longrightarrow 0 \quad \text{as} \quad t\longrightarrow\infty.$$

Since

$$V(t) \longrightarrow \infty \quad \text{as} \quad t \longrightarrow \infty \tag{3.52}$$

holds by (3.46), there exists a constant $T_b > 0$ satisfying (3.51). When $A < 0$, it follows from (3.40) that

$$v(t) \geq v(0) > 0 \quad \text{for} \quad 0 \leq t < T^* \quad \text{and} \quad v(t) \longrightarrow \infty \quad \text{as} \quad t \longrightarrow T^*,$$

where $T^* = -B^2/(2A)$. Since

$$V(t) = \int_0^t v(\tau)\, d\tau \longrightarrow \infty \quad \text{as} \quad t \longrightarrow T^*,$$

(3.51) holds for some $T_b (< T^*)$. In the case when $A = 0$, we have $v(t) = B/p^*$. Then, (3.52) also holds by (3.41), and then we find the existence of T_b.

(3.49) follows immediately from (3.40)–(3.42). We will show (3.50). It follows from (3.40)–(3.42) that

$$\begin{aligned} \ell''(t) &= a(s^*)v'(t) \\ &= -a(s^*)\frac{A}{p^*}\left(2\frac{A}{p^*}t + \left(\frac{B}{p^*}\right)^2\right)^{-3/2}. \end{aligned}$$

Since $a(s^*) > 0$ holds from Condition B, it suffices to show $A < 0$. We see from (3.43) and (2.13) that

$$\begin{aligned} A &\leq \int_{s^*}^1 \frac{-a'(\sigma)}{\lambda(s^*)}\, d\sigma - \frac{a(s^*)}{\lambda(0)} \\ &= a(s^*)\left\{\frac{1}{\lambda(s^*)} - \frac{1}{\lambda(0)}\right\}, \end{aligned}$$

which is negative by the assumption of the theorem, and the proof is complete.

REMARK 9. In the case of (2.8)–(2.9), our calculations by computer suggest that the constant A defined by (3.43) is negative if and only if $\mu > \mu^* \equiv 1.65\cdots$. Therefore, we may expect that $\ell'' > 0$ holds for $\mu > \mu^*$.

3.5. The existence of the steady state solutions

In this subsection, we consider the existence of steady state solutions of (2.17)–(2.19), which satisfy the following equations:

$$v\frac{d}{dx}f(s) - \varepsilon\frac{d}{dx}\left(d(s)\frac{d}{dx}s\right) = 0, \tag{3.53}$$

$$v = (p^* - c\varepsilon)\left(\int_0^1 \frac{dx}{\lambda(s)}\right)^{-1}, \tag{3.54}$$

(3.55) $s(0) = 1,\ s(x) > 0$ on $0 \leq x < x^*$ and $s(x) = 0$ on $x^* \leq x \leq 1,$

where $x^* \in (0, 1]$ is some constant to be determined.

The equations (3.53) and (3.54) are obtained from (2.17) and (2.18), respectively. We look for solutions which possess the interface $x = x^*$ in the interval $(0, 1]$.

THEOREM 6. *Assume* $\varepsilon > 0$. *Under Conditions A, B and C, the solution* $s(x)$ *and* v *of* (3.53)–(3.55) *exists if and only if* $p^* \leq 0$.

PROOF. Suppose that the solutions $s(x)$ and v of (3.53)–(3.55) exist. Then, from (3.53), we see that $vf(s) - \varepsilon(d(s)s')$ is a constant. Since $f(s(x^*)) = d(s(x^*)) = 0$ by (3.55) and (2.10), it follows that

$$f(s)(v - \varepsilon\phi(s)s') = vf(s) - \varepsilon(d(s)s') = 0. \tag{3.56}$$

By (2.10) and (3.55), $f(s) > 0$ holds for $x \in [0, x^*)$. Hence, from (3.56), we obtain $v - \varepsilon\phi(s)s' = 0$, and find that

$$s(x) = \Phi^{-1}\left(\frac{v}{\varepsilon}x + \Phi(1)\right) \quad x \in [0, x^*), \tag{3.57}$$

where

$$\Phi(s) = \int_0^s \Phi(\sigma)\, d\sigma.$$

We note that Φ^{-1} is well-defined, because Φ is a strictly monotone increasing function on $[0, 1]$ (see Condition A). Since $s(x^*) = 0$ and $x^* \in (0, 1]$, it follows from (3.57) that

$$x^* = -\frac{\varepsilon}{v}\Phi(1), \tag{3.58}$$

$$v \leq -\varepsilon\Phi(1). \tag{3.59}$$

On the other hand, by using (3.57) and (3.58), we have

$$\begin{aligned} v\left(\int_0^1 \frac{dx}{\lambda(s)}\right) &= v\int_0^{x^*} \frac{dx}{\lambda\left(\Phi^{-1}\left(\frac{v}{\varepsilon}x + \Phi(1)\right)\right)} + v\int_{x^*}^1 \frac{dx}{\lambda(0)} \\ &= -\varepsilon\int_0^1 \frac{\phi(\xi)}{\lambda(\xi)}\, d\xi + (v + \varepsilon\Phi(1))\frac{1}{\lambda(0)} \\ &= -c\varepsilon + \frac{v + \varepsilon\Phi(1)}{\lambda(0)}, \end{aligned}$$

where c is the constant defined by (2.20) and $\xi = \Phi^{-1}\left(\frac{v}{\varepsilon}x + \Phi(1)\right)$. From (3.54), it follows that

$$p^* = \frac{v + \varepsilon\Phi(1)}{\lambda(0)}, \tag{3.60}$$

which implies that $p^* \leq 0$ by (3.59).

Suppose that $p^* \leq 0$. We put $v = \lambda(0)p^* - \varepsilon\Phi(1)$ and define $s(x)$ by (3.57). Then $s(x)$ and v satisfy (3.53)–(3.55), which means the existence of the solution. Hence the proof of Theorem 6 is complete.

REMARK 10. From the proof, we find that $x^* = 1$ if and only if $p^* = 0$.

4. Two dimensional problem

In this section, we numerically study the behavior of the interface for the following two dimensional problem:

$$\frac{\partial}{\partial t}s + \nabla \cdot [vf] - \varepsilon\nabla \cdot [f\phi\nabla s] = 0 \quad \text{on } (x, y)\in\Omega,\ t > 0, \tag{4.1}$$

$$\nabla \cdot v = 0 \quad \text{on } (x, y)\in\Omega,\ t > 0, \tag{4.2}$$

$$v = -[\lambda\nabla p - \varepsilon\phi\nabla s] \quad \text{on } (x, y)\in\Omega,\ t > 0, \tag{4.3}$$

where $\Omega = (0, 1) \times (0, 1)$, under the boundary conditions

$$\frac{\partial s}{\partial y} = \frac{\partial p}{\partial y} = 0 \quad \text{on } (x, y)\in(0, 1) \times \{0, 1\},\ t > 0, \tag{4.4}$$

$$s = 1,\ p = p^* \quad \text{on } x = 0,\ y\in(0, 1),\ t > 0, \tag{4.5}$$

$$s = 0,\ p = 0 \quad \text{on } x = 1,\ y\in(0, 1),\ t > 0, \tag{4.6}$$

and under the initial condition

$$s(x, y, 0) = s^0(x, y) \quad \text{on } (x, y)\in\Omega, \tag{4.7}$$

where p^* is a given constant and s^0 satisfies $0 \leq s^0 \leq 1$.

The equations (4.1)–(4.3) are the same one as (2.5)–(2.7). In physical terms, the boundary conditions (4.5) and (4.6) express the injection of water with pressure p^* on $(0, y)$ $(0 < y < 1)$ and the production of oil on $(1, y)$ $(0 < y < 1)$, respectively.

The numerical scheme, which we use in this section, will be stated in Appendix, because it is lengthy. Throughout this section, the initial function takes

$$s^0(x, y) = \begin{cases} 1 - 10x, & \text{if } x < 0.1 \text{ and } |y - 0.5| < 0.1, \\ 0, & \text{otherwise.} \end{cases} \tag{4.8}$$

The first case is when $\varepsilon = 0$. Fig. 13 shows the numerical solution with $\mu = 0.5$. The numerical interface determined in a similar way to (3.12) is shown in Fig. 14. The perturbation given to the interface vanishes as t increases, which means that fingering instability does not occur. On the other hand, for $\mu = 20$, the perturbation grows up and forms fingers (see Figs. 15 and 16). Since $\mu = 10 \sim 20$ holds in the practical problems, 2a) stated in Section 1 seems to be true.

The second case is when $\varepsilon > 0$ and $p^* > 0$. Since we do not know the interface equation in this case, the interface-tracking scheme can not be constructed. From the profiles of numerical solutions, we find the behavior of the interface. Fig. 17 is the numerical solution with $\varepsilon = 0.01$ and $\mu = 20$. In the case where ε is small, the solution is similar to the one in Fig. 15, and shows the fingering instability. For $\varepsilon = 100$, the perturbation will vanish, and the interface is stabilized (Fig. 18). For $\varepsilon = 1$, the perturbation does not vanish (Fig. 19). From the above simulations, we may say that the

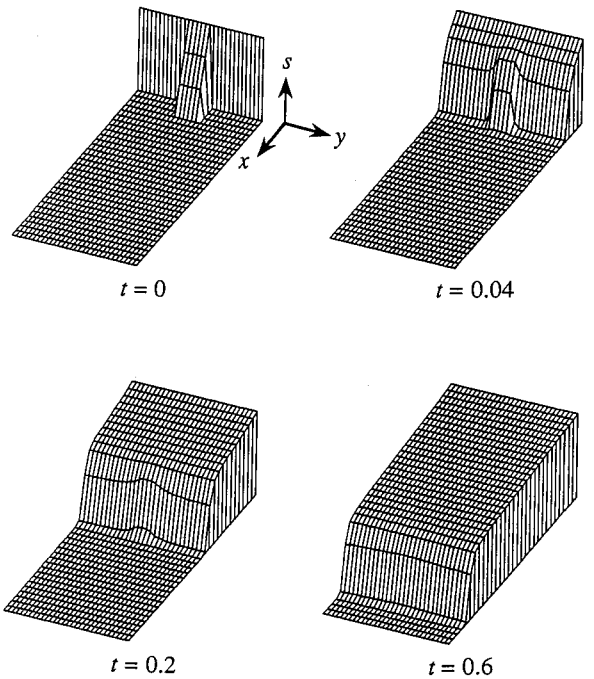

Fig. 13 Two dimensional numerical solution of (4.1)–(4.7) with $\varepsilon = 0$, $\mu = 0.5$, $p^* = 1$ and 50×50 mesh points.

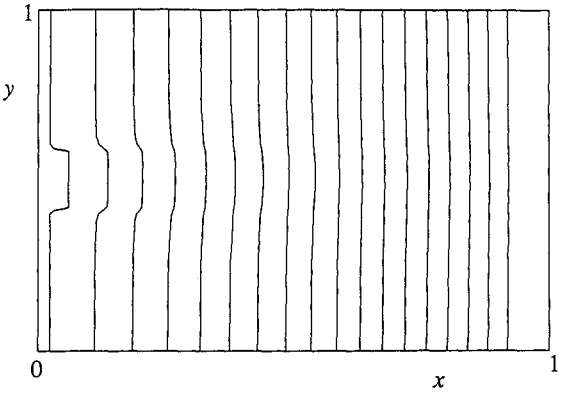

Fig. 14 Interface of numerical solution in Fig. 13 at $t = 0, 0.04, 0.08, \ldots, 0.68$.

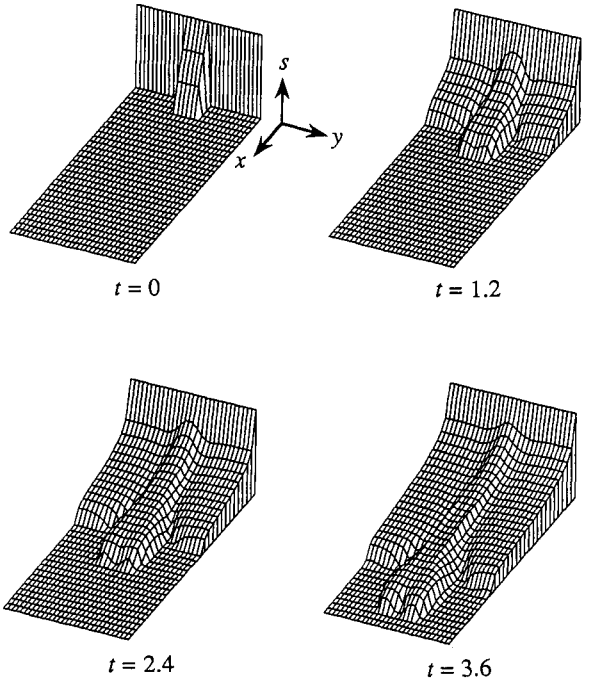

Fig. 15 Two dimensional numerical solution of (4.1)–(4.7) with $\varepsilon = 0$, $\mu = 20$, $p^* = 1$ and 100×100 mesh points.

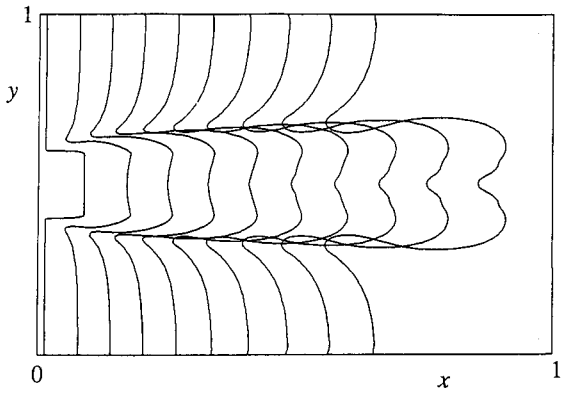

Fig. 16 Interface of numerical solution in Fig. 15 at $t = 0, 0.4, 0.8, \ldots, 3.6$.

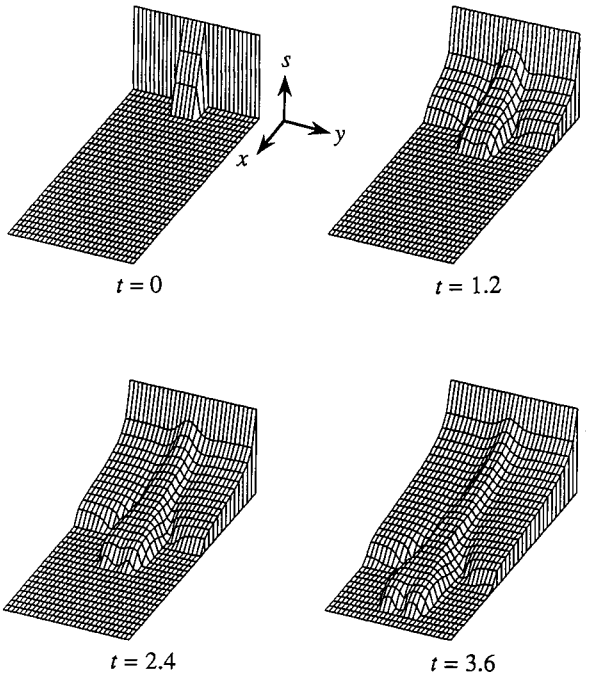

Fig. 17 Two dimensional numerical solution of (4.1)–(4.7) with $\varepsilon = 0.01$, $\mu = 20$, $p^* = 1$ and 100×100 mesh points.

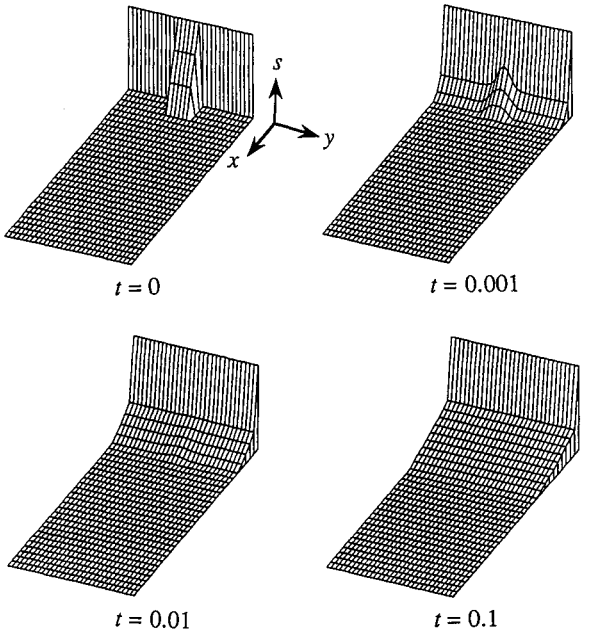

Fig. 18 Two dimensional numerical solution of (4.1)–(4.7) with $\varepsilon = 100$, $\mu = 20$, $p^* = 1$ and 50×50 mesh points.

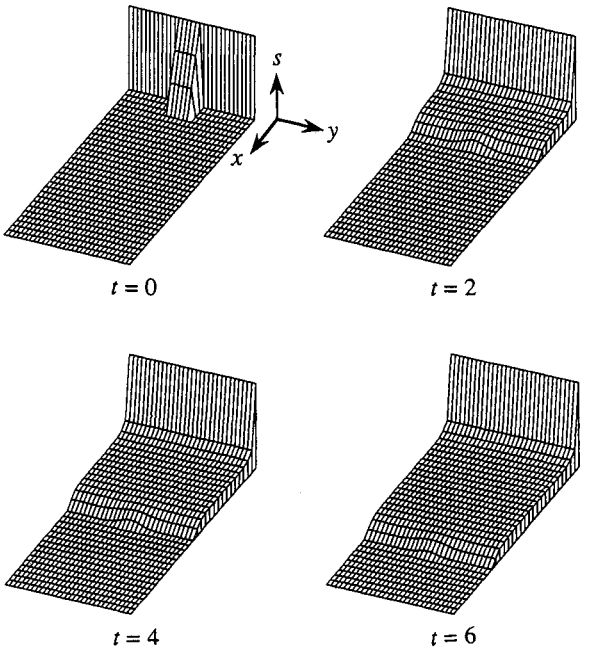

Fig. 19 Two dimensional numerical solution of (4.1)–(4.7) with $\varepsilon = 1$, $\mu = 20$, $p^* = 1$ and 50×50 mesh points.

interface is stable for large ε, which implies 2b). In this case, the numerical solutions become uniform with respect to y for each fixed x, and we expect that the interface reaches to $x = 1$ (see Theorem 4).

Finally, we consider when $p^* < 0$. Fig. 20 shows the numerical solution with $\varepsilon = 100$, $\mu = 20$ and $p^* = -50$. The solution also becomes uniform with respect to y. As was expected by Theorem 5, the interface will stop and never reach to the production well, and there is a steady state solution.

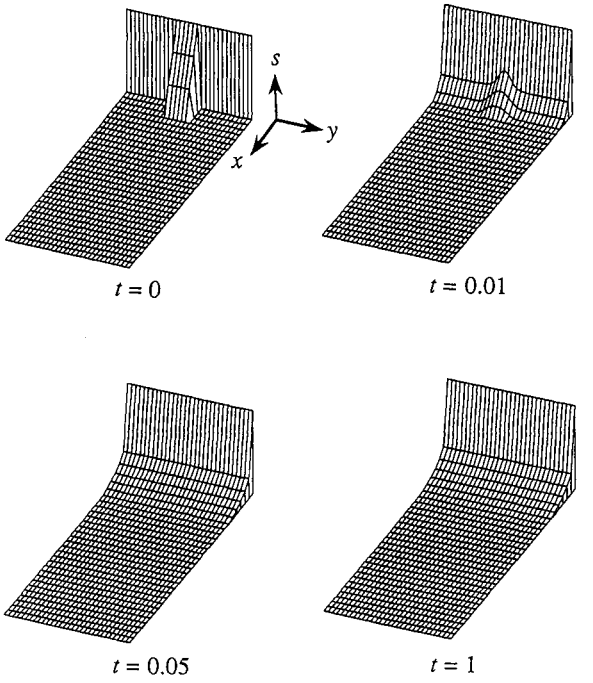

Fig. 20 Two dimensional numerical solution of (4.1)–(4.7) with $\varepsilon = 100$, $\mu = 20$, $p^* = -50$ and 50×50 mesh points.

5. Proofs of Theorems

5.1. Proof of Theorem 1

The proof will be done by induction on $n(\geq 0)$. We first prove (3.9).

For $n = 0$, (3.9) follows from (3.5). Suppose that (3.9) holds for some n. We will show

$$0 \leq s_j^{n+1} \leq 1 \quad (0 \leq j \leq J) \tag{5.1}$$

in the case where $v^n \geq 0$. When $j = 0$ and $j = J$, (5.1) follows at once from (3.4). In the following, we assume $1 \leq j \leq J - 1$. Putting

$$\theta_n = \frac{\Delta x |v^n| \, \| f' \|}{\Delta x |v^n| \, \| f' \| + 2\varepsilon \| d \|},$$

we obtain from (3.8)

$$\Delta t_n \leq \min \left\{ \frac{\Delta x}{|v^n| \, \| f' \|} \theta_n, \frac{\Delta x^2}{2\varepsilon \| d \|} (1 - \theta_n) \right\}. \tag{5.2}$$

It follows from (3.1) that

$$s_j^{n+1} = A_h s_j^n + B_h s_j^n, \tag{5.3}$$

where

$$A_h s_j^n = \theta_n s_j^n - \Delta t_n v^n \frac{f(s_j^n) - f(s_{j-1}^n)}{\Delta x}, \tag{5.4}$$

$$B_h s_j^n = (1 - \theta_n) s_j^n + \Delta t_n \varepsilon D_h s_j^n. \tag{5.5}$$

To prove (5.1), it suffices to prove

$$0 \leq A_h s_j^n \leq \theta_n, \tag{5.6}$$

$$0 \leq B_h s_j^n \leq 1 - \theta_n. \tag{5.7}$$

From (5.4), we have

$$\begin{aligned} A_h s_j^n &= \theta_n s_j^n - \frac{\Delta t_n}{\Delta x} v^n f'(\xi_j)(s_j^n - s_{j-1}^n) \\ &= \left[\theta_n - \frac{\Delta t_n}{\Delta x} v^n f'(\xi_j) \right] s_j^n + \frac{\Delta t_n}{\Delta x} v^n f'(\xi_j) s_{j-1}^n, \end{aligned} \tag{5.8}$$

where ξ_j is some number between s_j^n and s_{j-1}^n. Since (5.2) and Condition B yield

$$\theta_n - \frac{\Delta t_n}{\Delta x} v^n f'(\xi_j) \geq 0 \quad \text{and} \quad \frac{\Delta t_n}{\Delta x} v^n f'(\xi_j) \geq 0, \tag{5.9}$$

it follows that

$$\min \{ s_{j-1}^n, s_j^n \} \leq A_h s_j^n \leq \theta_n \max \{ s_{j-1}^n, s_j^n \}.$$

By the inductive hypothesis, we have (5.6).

Put

$$\alpha_k = \varepsilon \frac{\Delta t_n}{\Delta x^2} d\left(\frac{s_{k+1}^n + s_k^n}{2}\right) \quad (k = j-1, j).$$

Then we have from (5.5)

$$B_h s_j^n = \alpha_j s_{j+1}^n + (1 - \theta_n - \alpha_j - \alpha_{j-1}) s_j^n + \alpha_{j-1} s_{j-1}^n. \tag{5.10}$$

Since it follows from (5.2) that

$$0 \le \alpha_k \le \frac{1-\theta_n}{2} \quad (k = j-1, j), \tag{5.11}$$

(5.7) holds by the inductive hypothesis. Thus, (5.1) follows. In the case where $v^n < 0$, (5.1) can be similarly shown. Thus, the proof of (3.9) is complete.

Next, we will show (3.10). For $n = 0$, (3.10) is follows from the assumption of the theorem. Suppose that (3.10) holds for some n. We will prove

$$s_j^{n+1} \ge s_{j+1}^{n+1} \quad (0 \le j \le J-1) \tag{5.12}$$

in the case where $v^n \ge 0$. When $j = 0$ and $j = J-1$, (5.12) follows at once from (3.4) and (3.9). In the following, we assume $1 \le j \le J-2$. We have from (5.3), (5.8) and (5.10)

$$s_{j+1}^{n+1} - s_j^{n+1} = A s_{j+1}^n - A s_j^n + B s_{j+1}^n - B s_j^n,$$

$$\begin{aligned} A_h s_{j+1}^n - A_h s_j^n &= \left[\theta_n - \frac{\Delta t_n}{\Delta x} v^n f'(\xi_{j+1})\right] s_{j+1}^n + \frac{\Delta t_n}{\Delta x} v^n f'(\xi_{j+1}) s_j^n \\ &\quad - \left[\theta_n - \frac{\Delta t_n}{\Delta x} v^n f'(\xi_j)\right] s_j^n - \frac{\Delta t_n}{\Delta x} v^n f'(\xi_j) s_{j-1}^n \\ &= \left[\theta_n - \frac{\Delta t_n}{\Delta x} v^n f'(\xi_{j+1})\right](s_{j+1}^n - s_j^n) + \frac{\Delta t_n}{\Delta x} v^n f'(\xi_j)(s_j^n - s_{j-1}^n), \end{aligned}$$

$$\begin{aligned} B_h s_{j+1}^n - B_h s_j^n &= \alpha_{j+1} s_{j+2}^n + (1 - \theta_n - \alpha_j - \alpha_{j+1}) s_{j+1}^n + \alpha_j s_j^n \\ &\quad - \alpha_j s_{j+1}^n - (1 - \theta_n - \alpha_{j-1} - \alpha_j) s_j^n - \alpha_{j-1} s_{j-1}^n \\ &= \alpha_{j+1}(s_{j+2}^n - s_{j+1}^n) + (1 - \theta_n - 2\alpha_j)(s_{j+1}^n - s_j^n) + \alpha_{j-1}(s_j^n - s_{j-1}^n). \end{aligned}$$

Since

$$A_h s_{j+1}^n - A_h s_j^n \le 0 \quad \text{and} \quad B_h s_{j+1}^n - B_h s_j^n \le 0 \tag{5.13}$$

holds by (5.9), (5.11) and the inductive hypothesis, (5.12) follows. In the case where $v^n < 0$, (5.12) can be similarly shown and the proof of (3.10) is complete.

5.2. Proof of Theorem 2

Since Condition B implies that

$$\lambda(s) \leq \delta_1 \qquad \text{for all } s \in [0, 1]$$

holds for some constant $\delta_1 > 0$, we see from (3.3) that

$$|v^n| \leq |p^* - c\varepsilon|\,\delta_1.$$

Put

$$\delta = \frac{\Delta x^2}{\Delta x|p^* - c\varepsilon|\delta_1 \|f'\| + 2\varepsilon\|d\|}.$$

Then δ satisfies (3.11).

5.3. Proof of Theorem 3

The proof will be done by induction on $n(\geq 0)$. We first prove (3.9).

For $n = 0$, (3.9) follows from (3.5). Suppose that (3.9) holds for some n. We will show

$$0 \leq s_j^{n+1} \leq 1 \tag{5.14}$$

in the following cases:

Case(a). $0 \leq j \leq L_n - 1$; Case(b). $j = L_n$; Case(c). $L_n + 1 \leq j \leq L_{n+1}$; Case(d). $L_{n+1} + 1 \leq j \leq J$.

By the same argument as the one used in the proof of Theorem 1, (5.14) can be shown in Case(a). Consider Case(b). Assume $v^n \geq 0$. Let $\theta_n = \tau_2/(\tau_1 + \tau_2)$. Then we have from (3.31)

$$\Delta t_n \leq \min\{\theta_n \tau_1, (1 - \theta_n)\tau_2\}. \tag{5.15}$$

It follows from (3.20) that

$$s_L^{n+1} = A_h s_L^n + B_h' s_L^n,$$

where $L = L_n$, A_h is the operator defined by (5.4) and

$$B_h' s_L^n = (1 - \theta_n)s_L^n + \varepsilon \Delta t_n D_h' s_L^n.$$

By the same argument as the one used in the proof of (5.6), we have

$$0 \leq A_h s_L^n \leq \theta_n. \tag{5.16}$$

Putting

$$\alpha_{L-1}' = \Delta t_n \frac{2\varepsilon}{\Delta x(h + \Delta x)} d\left(\frac{s_L^n + s_{L-1}^n}{2}\right) \quad \text{and} \quad \alpha_L' = \Delta t_n \frac{2\varepsilon}{h(h + \Delta x)} d\left(\frac{s_L^n}{2}\right),$$

we obtain

$$B_h' s_L^n = (1 - \theta_n - \alpha_{L-1}' - \alpha_L')s_L^n + \alpha_{L-1}' s_{L-1}^n. \tag{5.17}$$

Since (3.34) and (5.15) imply

$$\alpha'_{L-1} + \alpha'_L = \frac{\Delta t_n}{\tau_2} \leq 1 - \theta_n, \quad \text{and} \quad \alpha'_{L-1} \geq 0, \tag{5.18}$$

it follows from (5.17) and the inductive hypothesis that

$$0 \leq B'_h s^n_L \leq 1 - \theta_n. \tag{5.19}$$

From (5.16) and (5.19), (5.14) holds. When $v^n < 0$, (5.14) can be similarly shown in this case. In Cases (c) and (d), (5.14) follows from (3.22) and (3.23), and the proof of (3.9) complete.

Next, we show (3.10). For $n = 0$, (3.10) follows from the assumption of the theorem. Suppose that (3.10) holds for some n. We will prove

$$s^{n+1}_j \geq s^{n+1}_{j+1} \tag{5.20}$$

in the following cases:

Case(a). $j = 0$; Case(b). $1 \leq j \leq L_n - 2$; Case(c). $j = L_n - 1$;
Case(d). $L_n \leq j \leq L_{n+1}$; Case(e). $L_{n+1} \leq j \leq J - 1$.

In Case(a), (5.20) follows from (3.9) and (3.25). By the same argument as the one used in the proof of Theorem 1, (5.20) can be also shown in Case(b). Consider Case(c). Assume $v^n \geq 0$. We have from (3.18) and (3.20)

$$s^{n+1}_L - s^{n+1}_{L-1} = A_h s^n_L - A_h s^n_{L-1} + B'_h s^n_L - B_h s^n_{L-1},$$

where A_h, B_h and B'_h are the operators defined by (5.4), (5.5) and (5.17), respectively, and $L = L_n$. We obtain

$$A_h s^n_L - A_h s^n_{L-1} \leq 0 \tag{5.21}$$

by the same argument as the one used in the proof of (5.13). It follows from (5.10) and (5.17) that

$$\begin{aligned} B'_h s^n_L - B_h s^n_{L-1} &= (1 - \theta_n - \alpha'_{L-1} - \alpha'_L) s^n_L + \alpha'_{L-1} s^n_{L-1} \\ &\quad - \alpha_L s^n_L - (1 - \theta_n - \alpha_{L-2} - \alpha_{L-1}) s^n_{L-1} - \alpha_{L-2} s^n_{L-2} \\ &= -\alpha'_L s^n_L + (1 - \theta_n - \alpha'_{L-1} - \alpha_L)(s^n_L - s^n_{L-1}) + \alpha_{L-1}(s^n_{L-1} - s^n_{L-2}). \end{aligned}$$

Since $h \leq \Delta x$ implies $\alpha_L \leq \alpha'_L$, (5.18) yields

$$1 - \theta_n - \alpha'_{L-1} - \alpha_L \geq 1 - \theta_n - \alpha'_{L-1} - \alpha'_L \geq 0.$$

Then, by the inductive hypothesis we obtain

$$B'_h s^n_L - B_h s^n_{L-1} \leq 0. \tag{5.22}$$

From (5.21) and (5.22), (5.20) follows. When $v^n < 0$, (5.20) can be similarly

shown in this case. In Cases (d) and (e), (5.20) follows from (3.22) and (3.23), and the proof of (3.39) is complete.

6. Appendix

In this appendix, we state the outline of the scheme of the two dimensional problem (4.1)–(4.7). In this problem, v depends on (x, y) in general, and it is not easy to eliminate p. To construct an approximation of p, we use

$$\nabla \cdot [\lambda \nabla p] = -\varepsilon \nabla \cdot [\phi \nabla s], \tag{6.1}$$

which is obtained by (4.2) and (4.3).

Let I and J be positive numbers and put $\Delta x = 1/I$ and $\Delta y = 1/J$. We determine $s^n_{i,j}$, which denotes the numerical approximation of s at $(x, y, t) = (i\Delta x, j\Delta y, t_n)$. For $n = 0$, put $t_0 = 0$, and $\{s^0_{i,j}\}_{0 \le i \le I, 0 \le j \le J}$ are determined by the initial function s^0. Assume that $\{s^n_{i,j}\}_{0 \le i \le I, 0 \le j \le J}$ and t_n are given. We will construct $\{s^{n+1}_{i,j}\}_{0 \le i \le I, 0 \le j \le J}$ and t_{n+1} by the following form:

$$s^{n+1}_{i,j} = (I_h + \varepsilon \Delta\tau_n D_h)^{\Delta t_n/\Delta\tau_n}(I_h + \Delta t_n C^y_h)(I_h + \Delta t_n C^x_h)s^n_{i,j}, \tag{6.2}$$

$$v^n_{i,j} = -[\lambda(s^n_{i,j})\tilde{\nabla} p^n_{i,j} - \varepsilon\phi(s^n_{i,j})\tilde{\nabla} s^n_{i,j}], \tag{6.3}$$

$$\tilde{\nabla} \cdot [\lambda(s^n_{i,j})\tilde{\nabla} p^n_{i,j}] = -\varepsilon \tilde{\nabla} \cdot [\phi(s^n_{i,j})\tilde{\nabla} s^n_{i,j}], \tag{6.4}$$

$$s^n_{0,j} = 1,\ s^n_{I,j} = 0 \quad (j = 0, 1, \ldots, J), \tag{6.5}$$

$$p^n_{0,j} = p^*,\ p^n_{I,j} = 0 \quad (j = 0, 1, \ldots, J), \tag{6.6}$$

$$s^n_{i,-1} = s^n_{i,1},\ s^n_{i,J+1} = s^n_{i,J-1} \quad (i = 0, 1, \ldots, I), \tag{6.7}$$

$$p^n_{i,-1} = p^n_{i,1},\ p^n_{i,J+1} = p^n_{i,J-1} \quad (i = 0, 1, \ldots, I), \tag{6.8}$$

$$t_{n+1} = t_n + \Delta t_n, \tag{6.9}$$

where $\tilde{\nabla}$, D_h, C^x_h and C^y_h are operators approximating ∇, $\nabla \cdot [f\phi\nabla]$, $-(u^n_{i,j} f)_x$ and $-(w^n_{i,j} f)_y$, respectively, $p^n_{i,j}$ and $v^n_{i,j} = {}^t(u^n_{i,j}, w^n_{i,j})$ are numerical approximations for p and v at $(x, y, t) = (i\Delta x, j\Delta y, t_n)$, respectively, and I_h is the identity operator.

(6.2) is constructed by splitting the equation (4.1). The equations (6.3) and (6.4) follow from (4.3) and (6.1), respectively. (6.5)–(6.8) are numerical boundary conditions obtained by (4.5)–(4.6), respectively. We note that (6.2) is a linear equation with respect to $\{p^n_{i,j}\}$.

The time step Δt_n is determined to satisfy the stability conditions for $I_h + \Delta t_n C^x_h$ and $I_h + \Delta t_n C^y_h$, that is

$$\Delta t_n \leq \min\left\{\frac{\Delta x}{|u^n|\,\|f'\|}, \frac{\Delta y}{|w^n|\,\|f'\|}\right\}.$$

We also determine $\Delta\tau_n$ satisfying the stability condition of $I_h + \varepsilon\Delta\tau_n D_h$, that is

$$\Delta\tau_n \leq \frac{\min\{\Delta x, \Delta y\}}{4\varepsilon\|d\|} \quad \text{and} \quad \Delta t_n/\Delta\tau_n \text{ is an integer.}$$

References

[1] J. Bear, Dynamics of Fluids in Porous Media, American Elsevier Publishing Company Inc., 1972.

[2] A. J. Chorin, The instability of fronts in a porous medium, Comm. Math. Phys., **91** (1983), 103–116.

[3] L. P. Dake, Fundamentals of Reservoir Engineering, Elsevier Science Publishing Company Inc., 1978.

[4] B. Engquist and S. Osher, Stable and entropy satisfying approximations for transonic flow calculations, Math. Comp., **34** (1980), 45–75.

[5] R. E. Ewing, The Mathematics of Reservoir Simulations, SIAM, 1983.

[6] W. E. Futzgibbon, Mathematical and Comptational Methods in Seismic Exploration and Reservoir Modeling, SIAM, 1986.

[7] B. H. Gilding, Properties of solutions of an equation in the theory of infiltration, Arch. Rat. Mech. Anal., **65** (1977), 203–225.

[8] J. Glimm, D. Marchesin and O. McBryan, Unstable fingers in two phase flow, Comm. Pure Appl. Math., **24** (1981), 53–75.

[9] P. D. Lax, Hyperbolic Systems of Conservation Laws and The Mathematical Theory of Shock Waves, SIAM, 1973.

[10] R. J. LeVeque, Numerical Methods for Conservation Laws, Birkhäuser Verlag, 1990.

[11] M. Mimura, T. Nakaki and K. Tomoeda, A numerical approach to interface curves for some nonlinear diffusion equations, Japan J. Appl. Math., **1** (1984), 93–139.

[12] K. Mochizuki and R. Suzuki, One-dimensional two-phase porous flow equations, Japan J. Appl. Math., **7** (1990), 277–300.

[13] T. Nakaki, Numerical interfaces in nonlinear diffusion equations with finite extinction phenomena, Hiroshima Math. J., **18** (1988), 373–397.

[14] S. Richardson, Hele Shaw flows with a free boundary produced by the injection of fluid into a narrow channel, J. Fluid Mech., **56** (1972), 609–618.

[15] A. E. Scheidegger, The Physics of Flow Through Porous Media, Third edition, University of Toronto Press, 1974.

[16] D. H. Sharp, An overview of Rayleigh-Taylor instability, Physica **12D** (1984), 3–18.

[17] J. Smoller, Shock Waves and Reaction-Diffusion Equations, Springer-Verlag, 1980.

[18] M. F. Wheeler, Numerical Simulation in Oil Recovery, Springer-Verlag, 1988.

Department of Mathematics,
Fukuoka University of Education
Munakata Fukuoka 811–41, *Japan*